In-line dielectric monitoring during extrusion of filled polymers

Anthony J. Bur[a] and Steven C. Roth
Polymers Division, National Institute of Standards and Technology, Gaithersburg, Maryland 20899-8542

Michael McBrearty
Chemical ElectroPhysics Corporation, Hockessin, Delaware 19707

(Received 18 December 2001; accepted for publication 25 February 2002)

Real-time monitoring of the dielectric properties of polymer melts and filled polymer melts has been carried out during extrusion. The measurements are obtained using a dielectric cell that is placed directly in line with the extruder machine. The dielectric cell consists of interdigitating electrodes that are deposited on the inside of a ceramic ring that is electrically insulated and temperature controlled to the set point of extrusion. As the processed resin passes through the ring, its permittivity and conductivity are measured. The spatial sensitivity of the cell was determined experimentally and was biased to the resin flowing near the electrodes. Using the spatial sensitivity function, we examined the time profile of the transition from one composition to another during extrusion. We demonstrate the operation of the cell during the processing of polystyrene filled with aluminum oxide and calcium carbonate and of polyethylene-ethyl vinyl acetate copolymer filled with montmorillonite clay. © *2002 American Institute of Physics.* [DOI: 10.1063/1.1470235]

I. INTRODUCTION

Monitoring of resin compounding is a significant challenge to the polymer processing industry because maintaining product quality requires that measurements of filler or additive concentration and the degree of mixing be carried out on a continuous basis. Often, these measurements are done off line, but real-time monitoring has the advantage of immediate scrutiny that allows detection of migration from steady state set points and observation of transition times from one composition to another as well as batch-to-batch differences. Monitoring in real time permits timely decisions regarding process machine set points. Monitoring techniques are of several types: spectroscopic such as infrared, optical such as optical transmission and fluorescence, ultrasonics, rheometry, and electrical such as dielectric measurements. Every monitoring technique has its advantages and disadvantages. Using several techniques in concert can yield complementary information that is not obtainable from one measuring technique alone. Dielectric measurements are particularly versatile because both permittivity and conductivity are measured as a function of frequency. Sensitivity to the polymer/filler composition can arise because of permittivity (dielectric constant) contrast between resin and filler or because of changes in conductivity that occur upon a change in filler concentration, and such changes can be accented by the frequency dependence. Measurements as a function of frequency yield information about dynamics of molecular dipoles and conducting ionic species and the influence of heterogeneous mixtures on bulk conductivity and permittivity.

Dielectric measurements have been employed as a tool by which to characterize polymer behavior from the earliest years of polymer science.[1,2] However, using dielectrics as a real-time monitoring tool is a relatively new technique, particularly for monitoring thermoplastics during extrusion processing.[3] One of the first demonstrations of dielectric monitoring employed a sensor with planar interdigitating electrodes to monitor epoxy curing.[4–7] The interdigitating design permits one sided sensing, i.e., measurements are made on specimens that are in contact with the sensing surface and do not require that the applied electric field extend through the bulk of the material to another electrode surface. The planar interdigitating sensor has been used in a number of applications, monitoring polymerization, resin curing, aging, and surface phenomena where the experiments were carried out under essentially quiescent conditions.[4–12] But, with the exception of the work reported in Ref. 3, an interdigitating sensor has not been used in situations that require mechanical robustness of the sensing surface such as monitoring filled resins during extrusion compounding.

An in-line dielectric sensor with parallel plates was used by Boersma and van Turnhout to monitor polymer blends compounded in a twin screw extruder.[13] In order to achieve reasonable capacitance and measurement sensitivity, the parallel electrodes, through which resin flowed, were separated by a small gap, 0.5 mm, thus creating a dielectric cell that acted as a slit die. At high shear rates, Boersma and van Turnhout noted that the dimensions of their dielectric cell/slit die were distorted by the high normal forces of resin flow, thus throwing the cell out of calibration. Problems associated with the parallel plate design can be avoided by using interdigitating electrodes.

The subject of this article is a robust dielectric cell with interdigitating electrodes that is used to monitor filled resins during extrusion processing. The cell has a ring configuration with the electrodes on the inside surface of the ring. As resin flows through the ring, it intercepts electric field lines that fringe between electrodes thereby permitting the determina-

[a]Electronic mail: anthony.bur@nist.gov

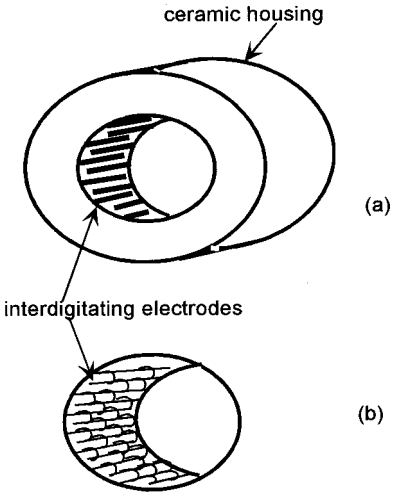

FIG. 1. (a) In-line dielectric cell with interdigitating electrodes in a ring ceramic housing; (b) fringing field between electrodes.

tion of its dielectric properties. We found that permittivity and conductivity measurements of resin melts can be used to quantify filler concentrations. Additive rules for the permittivity of two component systems are examined and procedures are given for predicting the precision of the method in prospective compounding applications. We also measured the spatial sensitivity of the sensor and used this information to profile transitions of resin composition during extrusion processing.

II. EXPERIMENTAL PROCEDURE

Some details of the design and construction of the dielectric sensor and the configuration of the electrodes were published earlier.[3] The core element of the sensor is a ceramic ring whose inside surface contains the interdigitating electrodes. Two sizes of ceramic ring have been used, the large cell: 7.6 cm outside diameter (o.d.)$\times$4.51 cm inside diameter (i.d.)$\times$3.8 cm long with 1.2 mm wide electrodes separated by 1.2 mm, and the small cell: 3.0 cm o.d. $\times$1.27 cm i.d.$\times$2.5 cm long with 0.33 mm electrodes separated by a 0.33 mm gap. The uncertainty in the above dimensions is one unit of the last significant figure. A sketch of the design is shown in Fig. 1.

The ceramic sensor core, onto which the electrodes are deposited, is contained in a cylindrical stainless steel housing with a thermally controlled heater band and an instrument port for a pressure/temperature transducer. The sensor and housing are designed to withstand pressures up to 21 MPa (3000 psi) and temperatures up to 400 °C. Electrical feedthroughs connect the electrodes to a computer controlled lock-in amplifier that applies a sinusoidal voltage and measures the resulting in-phase and out-of-phase currents. These signals are fed to the computer where a calculation of capacitance and resistance is made. Dielectric measurements are carried out over a frequency range of 500 Hz–10^5 Hz.

Accurate measurements of complex permittivity depend on accurate calibration of the cell over the temperature range of the experiments. An empty cell must measure a relative permittivity of one over the temperature range of interest, and the resistivity of the cell must be taken into account.

The measured capacitance C and resistance R can be expressed as

$$C=\varepsilon_0 g(\varepsilon'+\varepsilon'_{\mathrm{cer}}), \tag{1}$$

$$\frac{1}{R}=g(\sigma+\sigma_{\mathrm{cer}}), \tag{2}$$

where g is a geometrical constant (units in meters) that characterizes the sensitivity of the sensor, $\varepsilon_0=8.854\times10^{-12}$ F/m, ε' and σ are the relative permittivity and conductivity of the specimen, respectively, and $\varepsilon'_{\mathrm{cer}}$ and σ_{cer} are the relative permittivity and conductivity of the ceramic material of which the sensor body is constructed. The calibration quantities $\varepsilon'_{\mathrm{cer}}$ and σ_{cer} depend on the temperature and frequency while g is a constant. The imaginary part of the relative permittivity ε'' is related to the conductivity as

$$\varepsilon''=\frac{\sigma}{\omega\varepsilon_0}, \tag{3}$$

where ω is the radial frequency.

For the measurement, a 1 V root mean square (rms) sinusoidal voltage is applied to the electrodes and, using the lock-in amplifier, the current and phase angle are measured. The programmed computer then calculates C and R and uses Eqs. (1) and (2) to determine ε' and σ of the processed resin. The measurements are made at 16 point frequencies between 500 and 100 000 Hz in continually repeating sweeps that take about 2 min each. The frequency can be extended to lower frequencies (to 10^{-3} Hz), but acquisition of low frequency data consumes a large amount of time.

The cell is designed to attach to the output of a polymer extruder. For data reported here, we used a Haake rheocord model 9000, a twin screw extruder with corotating screws with an output cross section 19 mm in diameter. (Identification of a commercial product is made only to facilitate experimental reproducibility and to adequately describe the experimental procedure. In no case does it imply endorsement by NIST or that it is necessarily the best product for the experiment.) Between the extruder and dielectric cell, a flow adapter plate is used to match the diameter of the flow stream with that of the cell.

For the 45.1 mm cell, the diameter of the flow stream must expand upon exiting the extruder and for the small cell it contracts to a smaller diameter. The expansion (large cell) or contraction (small cell) has significant impact on the response time of the cell for a transition between one material composition and another. The response time to a change in composition in an expanding flow stream is much larger than that for a contracting flow stream.

We have used polystyrene (Dow Styron 613 26) and polyethylene (Dow Chemical PE 641) for the resin matrix with alumina powder filler that had average grain size of 10 μm (Acros) and with the calcium carbonate powder (Fisher Scientific). Premixing of resin pellets and powder was done in small batches of 100 g of resin to which was added powder, mixed by hand and placed in the feeder of the extruder. Also, data are presented for a mixture of polyethylene-ethyl

vinylacetate copolymer (Equistar UE630-000 with a 17% monomer fraction of vinyl acetate) (PE-EVA) and montmorillonite clay (Cloisite 15A from Southern Clay).

The standard uncertainty in the measurements that we report here is 0.01 for ε', 10^{-10} S/m for the conductivity, 1 °C for the temperature, and 70 kPa (10 psi) for the pressure.

A. Spatial sensitivity determination

Weak electric field lines fringe into the processed materials as they flow through the ring, but the sensitivity is confined to the near surface and the measurement is not fully representative of the entire sample. Neither cell is sensitive to the composition of the resin in the center of the ring, but the smaller cell has the potential for enhanced sensitivity to changes in filler composition because the flow stream is reduced in size as it enters the cell, causing higher shear stresses and dispersive mixing. This attribute is especially useful for monitoring the changes from composition A to composition B because, initially, composition B will appear at the center of the flow stream where the velocity is the highest. Over time, composition B migrates to the inside surface of the sensor ring, and this is achieved more rapidly with the smaller ring.

The strength of the fringing electric field, depicted in Fig. 1, falls off rapidly with the distance from the surface. For the planar configuration of interdigitating electrodes, the field strength falls off exponentially with a characteristic length that is approximately a third of the interelectrode spacing.[8,14] In the circular configuration of our sensor, the depth of field penetration depends on both the electrode spacing and the radius of curvature of the ring.

We have undertaken an experimental approach to determine the spatial sensitivity. The procedure involves inserting polymethyl methacrylate (PMMA) rods with a range of diameters into the center of the cell. This was done by placing the cell on the deck of a milling machine and using precision *xyz* adjustments to position the rod (held in the chuck) along the central axis of the cell. When the larger diameter rods are inserted into the sensing region of the cell, they intersect the fringing field between electrodes and increase the capacitance of the system.

Sensitivity can be expressed as relative permittivity versus the air gap between the PMMA rod and the surface of the cell. Data are shown in Fig. 2 for measurements made at 500 Hz. We see that there is a sharp rise in measured permittivity as the rod diameter approaches the dimension of the inside sensor diameter. In the experiment, zero gap is never achieved since there is always a small air gap between solid PMMA and the surface of the cell. In our analysis of the data, we account for this air gap by using the i.d. of the cell as a fitting parameter to optimize a polynomial fit to the data that must intersect the *y* axis (zero gap) at the relative permittivity of PMMA, 3.276, its value at room temperature and 500 Hz.[15] For the larger cell, optimal fit to the data [Fig. 2(a)] was obtained for a cell i.d. of 45.16 mm which is in good agreement with the fabricated i.d. of 45.1 mm. The curve shows that there is no sensitivity for gaps greater than 1 mm and that most of the sensitivity is confined to the region between 0 and 0.5 mm from the wall. The dashed curve is an exponential fit to the data and its characteristic decay dimension is 0.27 mm or 0.225 of the interelectrode spacing.

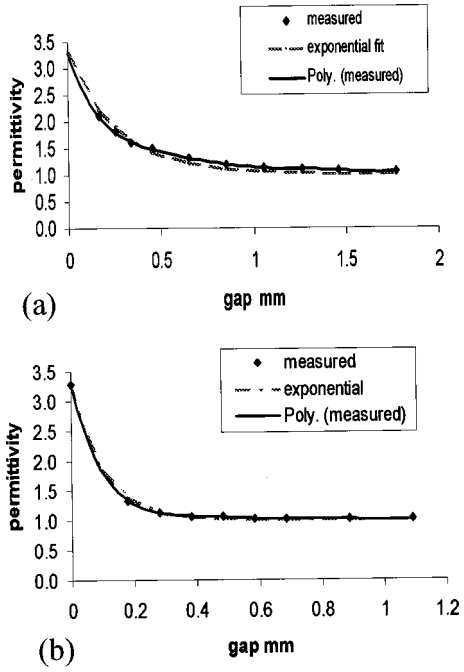

FIG. 2. Sensitivity curves for (a) the 45.1 mm i.d. cell and (b) the 12.7 mm diam cell. Poly refers to the polynomial fit of degree 5 to the experimental data points.

For the 12.7 mm diam cell [Fig. 2(b)], the sensitivity vanishes after a 0.4 mm gap so that material within the concentric central region with 11.9 mm diameter is not detected. Again, using the cell i.d. as the fitting parameter to optimize a polynomial fit to the data that must intercept the *y* axis at 3.276, the fit yields a cell i.d. of 12.65 mm which compares favorably the fabricated i.d. of 12.7 mm.[15] The dashed curve is the best exponential decay fit and it has a characteristic decay dimension of 0.10 mm, a third of the interelectrode distance. For both the large and small cells, the undetected region in the center of the flow steam is approximately 90% of the cross sectional area. For some applications, high surface sensitivity is an advantage since it can be used to monitor conditions at the wall.

The exponential fits to the data of Fig. 2 can be used as weighting functions to analyze flow patterns near the electrodes. For example, a compositional change in the resin mixture will first appear at the center of the flow stream. Over time the new composition spreads to the electrodes at the cell surface. Observed changes as a function of time, weighted by the sensitivity function, yield information about the duration and spatial range of the compositional change as it approaches the surface of the sensor.

III. RESULTS AND DISCUSSION

A. The mixture rule for dielectric materials

First we present dielectric measurements of polymer melts containing different fractions of filler. The objective is to examine the mixing rules and sensitivity to resin/filler

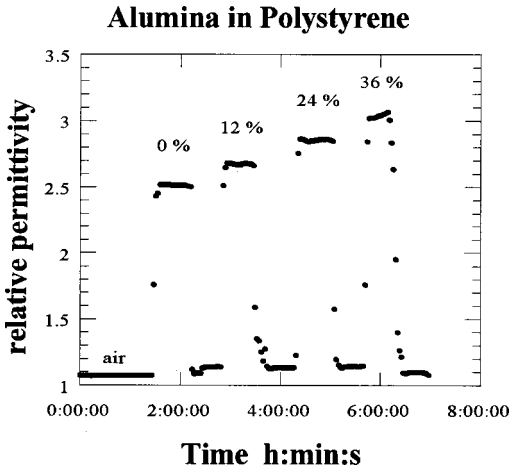

FIG. 3. Relative permittivity vs time for polystyrene filled with alumina. The percentages refer to the mass fraction of alumina in polystyrene.

composition ratios. In Fig. 3, data obtained from the 45.1 mm i.d. cell are plotted as permittivity versus time during the extrusion of polystyrene mixed with powdered alumina. The composition ranged from 0 to 0.36 mass fraction of alumina in the mixture and the extrusion was carried out at 180 °C. For this set of experiments, the cell was manually emptied of the old composition before a new composition was extruded into the cell. This was done because the transition time for one composition to completely replace the other in this cell took many hours. As noted above, the long transition time resulted from the slow displacement of the old composition at the electrodes with the new composition in an expanding flow stream.

Our purpose here is to apply dielectric mixture rules to the polystyrene/alumina data in order to develop the protocol for on-line composition determination using dielectric monitoring. Many mixture models have been proposed in the literature.[16] These models take into account how a second phase placed into a matrix of a first phase affects the internal field experienced by the minor phase. The larger the contrast in the permittivity between the two components, the larger the effect of adding the minor component.

While we have tried other mixing rules, the mixture rule that best satisfies our observations is the Landau–Lifshitz–Looyenga (LLL) mixing rule for homogeneous mixtures,

$$\varepsilon^{1/3}=\varphi_A\varepsilon_A^{1/3}+\phi_B\varepsilon_B^{1/3}, \tag{4}$$

where ϕ_A and ϕ_B are the volume fractions of primary material A and additive material B and ε_A and ε_B are their respective relative permittivities.[17,18] Equation (4) was used to analyze the permittivity data for mixtures of polystyrene with alumina and with calcium carbonate at 500 Hz, and the results are shown in Figs. 4 and 5. Both sets of data refer to extrusions carried out at 180 °C and 1 MPa. The straight line in the plots is a linear fit to our measurements. When the fit is extrapolated to 100% mass fraction filler, values for the relative permittivity of alumina, 9.10, and of calcium carbonate, 8.88, are obtained.

In general, a mixing rule based on the volume fraction of the components can be used to determine the volume fraction

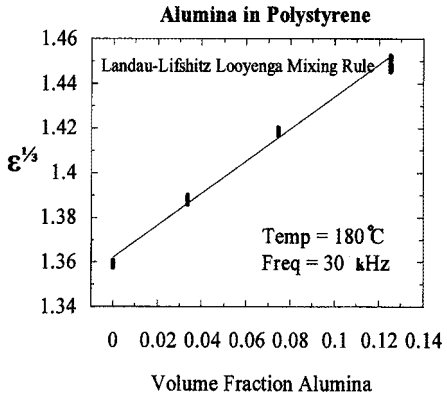

FIG. 4. Landau–Lifshitz–Loonenga mixing rule applied to alumina/polystyrene mixtures.

of the minor component from a measurement of the relative permittivity of the mixture,

$$\phi_B=\frac{f(\varepsilon)-f(\varepsilon_A)}{f(\varepsilon_B)-f(\varepsilon_A)}. \tag{5}$$

To estimate the accuracy in candidate applications, permittivities of polymers and additives can be measured or found in the literature. The precision of the determinations $\Delta\phi$ depends on the uncertainty $\Delta\varepsilon$ of the permittivity measurements (which for the in-line sensor is 0.01) and the magnitude of the contrast between the permittivity functions of the additive and primary materials as follows:

$$\Delta\phi_B=\frac{1}{|f(\varepsilon_B)-f(\varepsilon_A)|}\left.\frac{df}{d\epsilon}\right|_{\varepsilon_A}\Delta\varepsilon. \tag{6}$$

The precision of the composition determinations using the LLL mixture rule, presented in Figs. 4 and 5, was consistent with the uncertainty formula in Eq. (6) and its graphical presentation in Fig. 6. Here, the influence of dielectric contrast between mixture components is clearly delineated. For alumina in polystyrene, the formula indicates better than 0.5% volume fraction uncertainty and the data (Fig. 4) show that in the experiments 0.4% was achieved. Likewise for calcium carbonate in polystyrene the experimental uncertainty in the

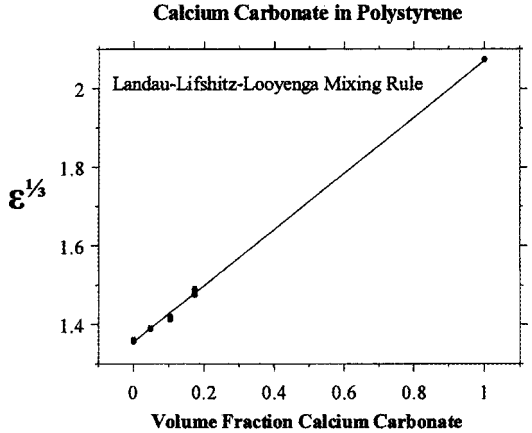

FIG. 5. Landau–Lifshitz–Loonenga mixing rule applied to calcium carbonate/polystyrene mixtures. The datum point for calcium carbonate is taken from the literature.

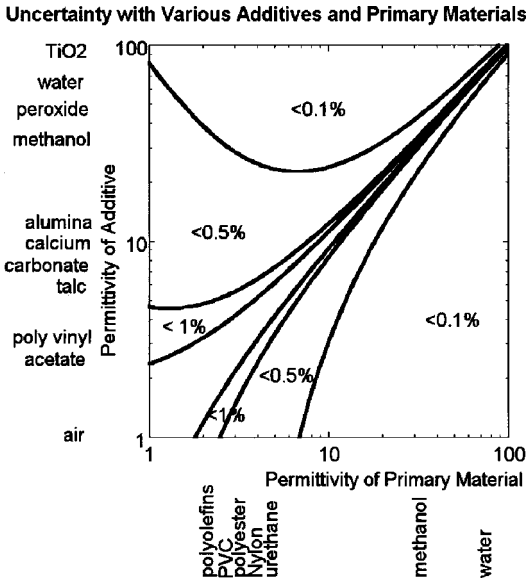

FIG. 6. Uncertainty chart as a function of additive and primary materials.

volume fraction determination was 0.4%. For real-time monitoring of steady state processing, the dielectric cell can be used to acquire continuous measurements at a single frequency every few seconds yielding nearly 100 measurements over a 3 min time span, thereby reducing the uncertainty by a factor of 10.

B. Monitoring compositional change

Real-time monitoring of extrusion during the transition from composition A to composition B is a primary goal of this measuring method. Above, we measured the spatial sensitivity of the cell in order to evaluate its performance and sensitivity to gross changes in the composition of the extrudate. The data for mixtures of polystyrene and alumina, shown in Fig. 3, were obtained only after manually removing the old composition near the electrode surface and allowing the new composition to flow into the cell and fill the region at the electrodes. If we had not manually intervened and removed material from the cell, a long wait would be necessary in order to see end of the transition. This is borne out by the data in Fig. 7 that were obtained using the 12.7 mm diam cell during extrusion of a polyethylene-ethylvinyl acetate copolymer mixed with clay while making a transition from 0%

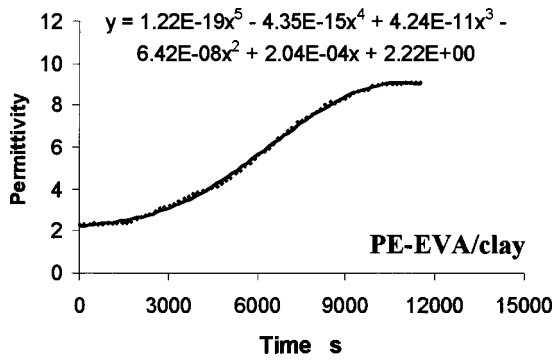

FIG. 7. Permittivity vs time during the transition from PE-EVA copolymer to a clay filled PE-EVA nanocomposite.

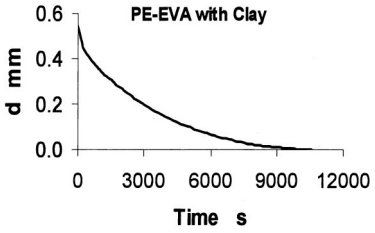

FIG. 8. Distance from the wall of the dielectric cell vs time of the boundary between PE-EVA and clay filled PE-EVA during extrusion.

mass fraction to 4.7% mass fraction of clay in the polymer. The observed transition time was approximately 2.5 h. The long transition time was an indication that the new composition initially flowed in the center of the flow stream and, over time, migrated toward the electrodes at the surface.

Using the sensitivity function derived from the data in Fig. 2, we are able to track the migration of the boundary between the two compositions as it moves toward the electrode surface. Consider the following normalized relationship,

$$\frac{\varepsilon(t)-\varepsilon_0}{\varepsilon_\infty-\varepsilon_0}=\frac{S(d)-S_0}{S_\infty-S_0}, \tag{7}$$

where $\varepsilon(t)$ is the relative permittivity of the composition at time t, ε_0 is the relative permittivity of the composition at the beginning of the transition, and ε_∞ is the relative permittivity at the end of the transition; $S(d)$ is a normalized sensitivity function derived from the data in Fig. 2, d is distance from the electrode surface, $S_0=0$ is the sensitivity at the beginning of the transition, and $S_\infty=1$ is the sensitivity at the end of the transition. The form of Eq. (7) is suggested by the smooth and continuous change in $\varepsilon(t)$. In using Eq. (7) to describe the transition, we assume that there is a sharp boundary between the two compositions at position d. From the data in Fig. 2, $S(d)$ can be given as

$$S(d)=e^{(d/\delta)}, \tag{8}$$

where $\delta=0.27$ mm for the large cell and $\delta=0.10$ mm for the small cell. Thus,

$$d(t)=-\delta\ln\left(\frac{\varepsilon(t)-\varepsilon_0}{\varepsilon_\infty-\varepsilon_0}\right). \tag{9}$$

By fitting the 500 Hz permittivity data in Fig. 7 with a polynomial function, we obtain

$$\varepsilon(t)=At^5+Bt^4+Ct^3+Dt^2+Et+F, \tag{10}$$

where A, B, C, D, E, and F are constant coefficients that are noted in Fig. 7. Using Eq. (10), we solve for $d(t)$ from Eq. (9). Figure 8 shows results of a calculation for $d(t)$, the position of the composition transition boundary between the PE-EVA copolymer and PE-EVA with 4.7% mass fraction of clay filler. The boundary moves slowly toward the electrode surface after 2 h of extrusion.

It is clear from the data in Fig. 2 that the characteristic length of sensitivity decay is a function of the interelectrode separation distance. By increasing the separation between electrodes, the fringe field will extend farther beyond the

surface, but at the same time the capacitance of the cell will decrease and affect the sensitivity of the overall measurement.

It is our plan to use this cell and varying designs of it to study polymer rheology at the surface. For example, wall slip may be preceded by extensional stress that orients the material at the surface and produces anisotropic dielectric properties. Other phenomena, such as the migration of polymer additives to the surface at high shear stress, may be detected in the same manner that we analyzed the migration of the composition boundary shown in Fig. 8.

[1] G. P. Simon, Mater. Forum **18**, 235 (1994).
[2] A. J. Bur, Polymer **26**, 963 (1985).
[3] S. Perusich and M. McBrearty, Polym. Eng. Sci. **40**, 214 (2000).
[4] D. Kranbuehl, S. Delos, E. Yi, J. Mayer, T. Jarvie, W. Winfree, and T. Hou, Polym. Eng. Sci. **26**, 338 (1986).
[5] D. Kranbuehl, S. Delos, M. Hoff, P. Haverty, W. Freeman, R. Hoffman, and J. Godfrey, Polym. Eng. Sci. **25**, 285 (1989).
[6] S. D. Senturia, N. F. Sheppard, H. L. Lee, and D. R. Day, J. Adhes. **15**, 69 (1982).
[7] N. F. Sheppard, D. R. Day, and H. L. Lee, Sens. Actuators **2**, 263 (1982).
[8] M. C. Zaretsky, P. Li, and J. R. Melcher, IEEE Trans. Electr. Insul. **24**, 1159 (1989).
[9] J. Fodor and D. A. Hill, Macromolecules **25**, 3511 (1992).
[10] D. R. Day, D. D. Sheppard, and K. J. Craven, Polym. Eng. Sci. **32**, 524 (1992).
[11] D. J. Melotik, M. Czaplicki, T. J. Whalen, and D. R. Day, Thermochim. Acta **217**, 251 (1993).
[12] D. D. Sheppard, J. Coat. Technol. **68**, 99 (1996).
[13] A. Boersma and J. van Turnhout, Polymer **40**, 5023 (1999).
[14] M. Zarestsky, L. Mouayad, and J. R. Melcher, IEEE Trans. Electr. Insul. **23**, 897 (1988).
[15] M. G. Broadhurst and A. J. Bur, J. Res. Natl. Bur. Stand., Sect. C **69**, 165 (1965).
[16] G. Banhegyi, Colloid Polym. Sci. **264**, 1030 (1986).
[17] H. Looyenga, Physica (Amsterdam) **31**, 401 (1965).
[18] L. D. Landau and E. M. Lifshiftz, *Electrodynamics of Continuous Media* (Pergamon, London, 1960), p. 46.